HHS Public Access

Author manuscript

Oral Oncol. Author manuscript; available in PMC 2023 December 01.

Published in final edited form as:

Oral Oncol. 2022 December ; 135: 106232. doi:10.1016/j.oraloncology.2022.106232.

Mildly dysplastic oral lesions with optically-detectable abnormalities share genetic similarities with severely dysplastic lesions

David R. Brenes[a,*,1], **Allison J. Nipper**[b,1], **Melody T. Tan**[a], **Frederico O. Gleber-Netto**[b], **Richard A. Schwarz**[a], **Curtis R. Pickering**[b], **Michelle D. Williams**[c], **Nadarajah Vigneswaran**[d], **Ann M. Gillenwater**[b], **Andrew G. Sikora**[b,2], **Rebecca R. Richards-Kortum**[a,*,2]

[a]Rice University, Department of Bioengineering MS-142, 6100 Main St., Houston, TX 77005, USA

[b]The University of Texas MD Anderson Cancer Center, Department of Head & Neck Surgery, 1400 Pressler Street, Houston, TX 77030, USA

[c]The University of Texas MD Anderson Cancer Center, Department of Anatomical Pathology, 1515 Holcombe Blvd, Houston, TX 77030, USA

[d]The University of Texas Health School of Dentistry, Department of Diagnostic and Biomedical Sciences, 7500 Cambridge St., Houston, TX 77054, USA

Abstract

Objective: Optical imaging studies of oral premalignant lesions have shown that optical markers, including loss of autofluorescence and altered morphology of epithelial cell nuclei, are predictive of high-grade pathology. While these optical markers are consistently positive in lesions with moderate/severe dysplasia or cancer, they are positive only in a subset of lesions with mild dysplasia. This study compared the gene expression profiles of lesions with mild dysplasia (stratified by optical marker status) to lesions with severe dysplasia and without dysplasia.

Materials and methods: Forty oral lesions imaged in patients undergoing oral surgery were analyzed: nine without dysplasia, nine with severe dysplasia, and 22 with mild dysplasia. Samples were submitted for high throughput gene expression analysis.

Results: The analysis revealed 116 genes differentially expressed among sites without dysplasia and sites with severe dysplasia; 50 were correlated with an optical marker quantifying altered nuclear morphology. Ten of 11 sites with mild dysplasia and positive optical markers (91%) had

*Corresponding authors. drb12@rice.edu (D.R. Brenes).
[1]David R. Brenes and Allison J. Nipper both contributed equally to this work.
[2]Andrew G. Sikora and Rebecca R. Richards Kortum both contributed equally to this work.

Declaration of Competing Interest

The authors declare the following financial interests/personal relationships which may be considered as potential competing interests: RR Richards-Kortum, AM Gillenwater, and RA Schwarz are recipients of licensing fees for intellectual property licensed from the University of Texas at Austin by Remicalm LLC. All other authors disclosed no potential conflicts of interest relevant to this publication.

Appendix A. Supplementary data

Supplementary data to this article can be found online at https://doi.org/10.1016/j.oraloncology.2022.106232.

gene expression similar to sites with severe dysplasia. Nine of 11 sites with mild dysplasia and negative optical markers (82%) had similar gene expression as sites without dysplasia.

Conclusion: This study suggests that optical imaging may help identify patients with mild dysplasia who require more intensive clinical follow-up. If validated, this would represent a significant advance in patient care for patients with oral premalignant lesions.

Keywords

Oral cancer; Gene expression analysis; Oral lesion; Dysplasia; Optical imaging

Introduction

Each year, over 350,000 people worldwide are diagnosed with cancers of the oral cavity and pharynx [1]. Around 60% of cases are diagnosed at late stages, usually due to metastasis to regional lymph nodes [2]. Oral cancer survival decreases with late-stage diagnosis. Five-year relative survival rates are estimated to drop from 84% for cancers diagnosed at a localized stage to 62% for those diagnosed after regional metastasis and to 39% for those diagnosed after distant metastasis [2]. These differences in survival rates underscore the importance of early detection and treatment of oral cancer and its precursors.

Many patients develop oral mucosal lesions, often termed oral premalignant lesions (OPLs) such as leukoplakia, prior to development of oral cancer. There are currently no reliable methods to determine which patients with OPLs are at highest risk to develop oral cancer. Pathologic identification of dysplasia in OPLs has been identified as a risk factor for oral cancer development [3]. One study by Warnakulasuriya et al. indicated that 5% of lesions with mild dysplasia, 16% of lesions with moderate dysplasia, and 27% of lesions with severe dysplasia undergo eventual malignant transformation [3]. Typically, lesions with moderate to severe dysplasia are treated with surgical resection, but it is challenging to manage patients with mild dysplasia [4,5].

The standard of care for detection of oral cancer and precancer is a conventional oral examination which includes visual and tactile assessment of the oral cavity with biopsy of suspicious lesions [6]. Due to limitations of efficacy of standard oral examination, several diagnostic adjuncts to improve early detection of oral cancer and precancer have been developed [7]. Validation of these new imaging technologies is limited due to the inability to reliably predict oral cancer risk based on standard clinical and pathologic examination, especially for mild dysplasia.

Several studies have examined whether genetic, molecular, or optical markers can help identify dysplastic oral lesions at highest risk of progression. Because optical markers can be assessed non-invasively at the point of care, they are particularly interesting. Previous studies have suggested that optical markers may help assess lesion risk *in vivo* and may indicate underlying carcinogenic alterations in areas that are clinically occult or do not yet exhibit histopathologic changes [8–11]. In a study of patients undergoing surgery for oral cancer, Poh et al. identified coincident loss of fluorescence beyond clinically visible tumors and loss of heterozygosity on chromosomes 3p, 9p, and 17p [12]. Optical spectroscopy

has shown promise in detecting field cancerization in the buccal mucosa of patients with esophageal squamous cell cancer [13]. A study of multimodal optical imaging found that optical markers could identify sites with moderate and severe dysplasia as well as 87% of sites with mild dysplasia that overexpress molecular markers associated with cancer progression [8].

Probing the relationship between changes in optical markers and altered expression of cancer-related genes could help develop better tools to assess the risk of potentially premalignant oral lesions, particularly those with mild dysplasia. Genes of interest comprise those involved in the pathways of the hallmarks of cancer, including sustaining proliferative signaling, evading growth suppressors, activating invasion and metastasis, enabling replicative immortality, inducing angiogenesis, and resisting cell death [14]. Gene expression analysis has been facilitated by advances in targeted high throughput sequencing techniques that allow thousands of genes to be screened per specimen. Commonly used platforms for high throughput analysis include the EdgeSeq system utilized in this study (HTG Molecular Diagnostics, Inc.) [15–17]. Here, we present a study that explores relationships between changes in optical markers and changes in gene expression of oral potentially premalignant lesions with histopathologically confirmed mild dysplasia.

Materials and methods

Study population

The study was conducted under protocols approved by the Institutional Review Boards of the University of Texas MD Anderson Cancer Center (Houston, TX) and Rice University (Houston, TX). Patients above the age of 18 scheduled for surgical resection of clinically visible oral lesions were eligible to participate. Patients were enrolled and treated between May 2015 and March 2019. Written informed consent was obtained from all patients prior to participation.

Imaging systems

Oral multimodal imaging was performed *in vivo* to obtain white light and autofluorescence images of lesions and high-resolution images of nuclear morphometry within lesions, using a system previously described [8,9,18,19]. Briefly, the handheld widefield imaging system is operated like a camera to capture images from a 4.5 cm diameter field of view with white light and 405 nm illumination [9,19]. A high-resolution microendoscope (HRME) is used to capture images from a 790 μm field of view following topical application of proflavine, a fluorescent antiseptic that stains cell nuclei [19]. All images are displayed in real-time on a tablet that controls the system.

Study methods

Patients undergoing surgery were imaged at the beginning of the scheduled surgery while under general anesthesia. The surgeon first conducted a standard white light examination to select imaging sites and provide a clinical impression of normal, abnormal, not suspicious (low risk), abnormal suspicious (high risk), or cancer for each site. The operating room lights were dimmed, and autofluorescence images were collected from each site. Proflavine

solution (0.01% w/v) was topically applied to each site using a cotton-tipped applicator immediately before high-resolution imaging. The surgeon then placed the high-resolution microendoscope in contact with each lesion to acquire high-resolution images. Imaged sites were then photographed and biopsied using a 4-mm punch biopsy or excised as part of the surgical specimen, according to the standard of care.

Pathology processing and review

Biopsy and surgical specimens were sectioned, processed as frozen section and/or formalin-fixed paraffin-embedded (FFPE) slides, and stained with hematoxylin and eosin (H&E) dyes, according to the standard of care. The histologic sections corresponding to each of the imaged sites were evaluated by the study pathologist and graded as no dysplasia, mild dysplasia, moderate dysplasia, severe dysplasia, or cancer using the World Health Organization classification system [20].

Selection of sites for analysis

Data from 77 patients were reviewed and sites were selected for combined analysis of optical markers and gene expression according to the following criteria: 1) no clinical evidence of lichen planus; 2) the full set of optical data (autofluorescence and high-resolution images) was available; 3) the corresponding histopathologic diagnosis was no dysplasia, mild dysplasia, or severe dysplasia; 4) there was sufficient remaining banked FFPE tissue to process three unstained slides with a total 6 mm^2 of the target region for gene analysis; and 5) tissue was collected from the ventral or lateral tongue. All sites that met the inclusion criteria were included in the analysis set.

Quantification of optical markers

For each site imaged, two optical markers were calculated. First, the normalized ratio of red-to-green autofluorescence was calculated as previously described (19). Briefly, the ratio of red-to-green autofluorescence intensity was first calculated from a 17-pixel diameter circle corresponding to the location of the histologic diagnosis; this was normalized by the red-to-green autofluorescence intensity ratio from a 65 × 65-pixel square ROI, selected by an automated algorithm. Second, the number of abnormal nuclei per unit area was calculated from the high-resolution image corresponding to the location of the histologic diagnosis using an automated process previously described [9,19,21]. Briefly, nuclear area and eccentricity were calculated for each nucleus in the image and used to determine the total number of abnormal nuclei per unit area [19].

Optical markers of sites with no dysplasia and sites with severe dysplasia were compared and nearest centroid classification was used to define a decision boundary between the two groups. The decision boundary was used to classify sites with mild dysplasia as optical marker positive or optical marker negative.

Quantification of gene expression

The study pathologist annotated the area of interest for each site on the H&E-stained slide. These annotations were manually transferred to unstained FFPE slides using a permanent marker to circle the target region. The unstained FFPE slides were shipped to HTG

Molecular Diagnostics, Inc. (Tucson, AZ) for microdissection of FFPE sample material and HTG EdgeSeq processing. The HTG EdgeSeq Oncology Biomarker Panel assay was used for the quantitative detection of 2,549 cancer-related genes. The quality control thresholds established by HTG Molecular Diagnostics, Inc. were used, by which sites with greater than 40% read depth relative to the positive control probes, fewer than 1.5 million total counts, or under 0.10 relative standard deviation of expression variability were excluded from subsequent analysis (HTG Molecular Diagnostics, Inc.). The multi-tissue controls were also applied. Numerical data indicating relative gene expression levels were returned from HTG Molecular Diagnostics, Inc.

Differential gene expression analysis

Differential expression analysis was conducted to identify genes upregulated and downregulated between sites with no dysplasia and sites with severe dysplasia. The analysis was performed using the HTG EdgeSeq Reveal platform to implement the edgeR method described by McCarthy et al. [22]. To account for multiple significance testing and control the false discovery rate, the Benjamini and Hochberg method was used to implement a Bonferroni-type correction to generate adjusted p-values for the analysis [23]. An adjusted p-value of 0.01 was used as the cutoff to identify genes with a significantly modulated expression between no dysplasia and severe dysplasia sites.

Joint analysis of optical markers and gene expression

Heat maps were used to visualize hierarchical clustering analysis of the significantly modulated genes identified from the differential expression analysis. JMP Pro 15 (SAS) was used to perform the hierarchical clustering analysis and generate the heat maps, where samples and probes were grouped. Gene expression was represented on a color scale normalized by the range of expression for each gene. First, gene expression levels from sites with no dysplasia and sites with severe dysplasia were mapped to confirm separation in gene expression between the groups. Subsequently, gene expression levels from all sites were mapped to identify clustering trends of sites with mild dysplasia that were optical marker negative and sites with mild dysplasia that were optical marker positive.

Pearson correlation was used to identify a subset of differentially expressed genes between sites with no dysplasia and sites with severe dysplasia that were strongly correlated to optical marker values. Principal component analysis (PCA) was applied to the subset of strongly correlated genes to determine whether they adequately represented the gene expression differences between sites with no dysplasia and sites with severe dysplasia. Nearest centroid classification used the PCA two-dimensional embedding of sites with no dysplasia and sites with severe dysplasia to define a boundary between the two groups. This boundary was then applied to PCA embeddings of sites with mild dysplasia. The ability of this boundary to separate sites with mild dysplasia based on their optical marker categorization (optical marker negative or optical marker positive) was evaluated.

Gene set enrichment on the strongly correlated genes was performed using Metascape [24] with all available pathways as of May 10, 2022. All other settings were default. Top terms from GO Biological Processes and Reactome Pathways categories were identified.

Results

Data selection

From the 77 patients reviewed, 22 sites with mild dysplasia met the inclusion criteria and were included in the analysis set. Nine sites with no dysplasia and nine sites with severe dysplasia met the inclusion criteria and were also included. Table 1 summarizes the characteristics of the 40 selected sites. The clinical impression was ‘normal’ for five mild dysplasia sites, ‘abnormal, not suspicious’ for six sites, ‘abnormal suspicious’ for nine sites, and ‘cancer’ for two sites. The clinical impression was ‘normal’ or ‘abnormal, not suspicious’ for all sites with no dysplasia. Clinical impressions for the sites with severe dysplasia were ‘normal’ for one site and ‘abnormal suspicious’ for eight sites. All sites were located in either the ventral or lateral tongue (Supplementary Table 1).

Multimodal imaging

Fig. 1 shows representative images from two patients with lesions on the ventral tongue. The clinical impression for both sites was ‘abnormal, not suspicious’, and the histologic diagnosis was mild dysplasia. Despite similar clinical impressions and histologic diagnoses, the optical markers of the two sites differed, with one showing an elevated red-to-green autofluorescence ratio and a high number of abnormal nuclei per unit area.

Fig. 2 characterizes all sites based on their optical markers. On average, sites with no dysplasia had lower values of optical markers than sites with severe dysplasia. Fig. 2b shows the nearest centroid classification decision boundary that separated sites with no dysplasia and sites with severe dysplasia based on the value of their optical markers. The decision boundary was used to classify sites with mild dysplasia into two categories: 1) optical marker positive and 2) optical marker negative (Fig. 2b). Of the 22 sites with mild dysplasia, 11 were identified as optical marker negative, and 11 were identified as optical marker positive. Fig. 2c shows the distribution of histologic diagnoses for sites that were optical marker positive or negative.

Gene expression analysis

All sites passed each post-sequencing quality control threshold and were included in the gene expression analysis. The multi-tissue lysate controls included by HTG Molecular Diagnostics, Inc. clustered closely together, as expected (data not shown). One hundred sixteen genes were differentially expressed between sites with no dysplasia and sites with severe dysplasia (adjusted p value < 0.01). The list of significantly differentially expressed genes with mean normalized values, fold change, p-values, and adjusted p-values can be found in **Supplementary Table 2**. Hierarchical clustering analysis of the 116 differentially expressed genes was used to examine the gene expression similarities between sites with: no dysplasia, severe dysplasia, mild dysplasia optical marker negative, and mild dysplasia optical marker positive. Fig. 3 shows that the gene expression of sites with mild dysplasia and positive optical markers clustered among sites with severe dysplasia. Sites with mild dysplasia and negative optical markers had a variable expression profile, clustering among sites with no dysplasia and sites with mild dysplasia and positive optical markers.

Joint optical marker and gene expression analysis

We analyzed associations between differentially expressed genes and optical marker values to determine if differential gene expression underlies variance in optical imaging metrics. The number of abnormal nuclei/mm2 and normalized R:G autofluorescence ratio were analyzed in relation to each of the 116 genes differentially expressed between groups of sites with no dysplasia and with severe dysplasia (Fig. 4a). Genes with a correlation coefficient ≤ -0.4 or ≥ 0.4 were considered strongly correlated with an imaging metric. By this calculation, 50 differentially expressed genes strongly correlated with the optical marker characterizing the number of abnormal nuclei. None of the differentially expressed genes strongly correlated with the normalized R: G autofluorescence ratio. A principal component analysis was performed on the 50 differentially expressed genes associated with the number of abnormal nuclei to evaluate whether sites with no dysplasia and sites with severe dysplasia could be distinguished based on differences in expression for this subset of genes (Fig. 4b). The nearest centroid classifier adequately separated sites with no dysplasia and severe dysplasia, misclassifying only one site with no dysplasia and one site with severe dysplasia. When this decision boundary was applied to sites with mild dysplasia, the sites were separated into two groups: one containing mainly mild dysplasia with positive optical markers, and one containing mild mainly dysplasia sites with negative optical markers (Fig. 4c). Ten of 11 sites with mild dysplasia and positive optical markers (91%) had similar gene expression as sites with severe dysplasia. Nine of 11 sites with mild dysplasia and negative optical markers (82%) had similar gene expression as sites without dysplasia (Fig. 4d).

Metascape analysis (Fig. 5) of the 50 differentially expressed genes revealed these genes are part of pathways involved in positive regulation of cell cycle, nuclear division, signaling by receptor tyrosine kinases, and positive regulation of the apoptotic process.

Discussion

Under the standard of care, the optimal management of oral pre-cancers with mild dysplasia is unclear, since only a small percentage of these sites undergo malignant transformation, but the impact of lesions which do progress can be devastating. Patients with mild dysplasia are often kept under surveillance with the option of re-biopsy when evidence of progression by visual inspection is found. However, dysplasia grading alone should not be used as an only indicator for treatment. A recent review on oral epithelial dysplasia advocated that mild dysplasia with lichenoid changes within epithelial and connective tissue interface and/or verrucous architecture merit higher grades because of their higher risk of malignant transformation [25]. Similarly, molecular biomarker data could provide valuable insights into underlying genetic changes that inform the assessment of the risk of progression of lesions with mild dysplasia risk; however, invasive biopsies are required for molecular biomarker detection. In contrast, optical imaging markers may be measured non-invasively at the point of care to help identify mild dysplasia lesions at high risk of progression.

While previous studies have demonstrated that autofluorescence imaging and high-resolution imaging can discriminate between non-dysplastic and dysplastic sites, attempts to use optical imaging to classify sites with mild dysplasia have been less conclusive [8,9]. In these studies, some sites with mild dysplasia were classified as non-dysplastic while others

had optical properties more similar to sites with severe dysplasia. Further exploration was needed to better understand whether changes in optical markers for sites with mild dysplasia were associated with the risk of progression.

This study was designed to explore relationships between optical markers and oncology-related gene expression in sites with mild dysplasia. Differential expression analysis identified 116 genes significantly modulated between samples with severe dysplasia and no dysplasia. Pathway analysis indicated that the differentially expressed genes were largely related to positive regulation of cell cycle, nuclear division, signaling by receptor tyrosine kinases, and positive regulation of the apoptotic process.

To minimize sample variation driven by the anatomic location of source tissue, tissue collection sites were restricted to the ventral or lateral tongue. Further studies are needed to reveal if optical markers are associated with similar changes to gene expression at other anatomic sites in the oral cavity.

Results of this study support the use of optical markers captured by high-resolution imaging to supplement pathology diagnosis in risk stratification of oral lesions. Our finding that lesions with mild dysplasia and positive optical markers have a similar gene expression profile to severe dysplasia sites, supports our hypothesis that optical imaging characteristics reflect the underlying biology of these lesions. This subset of sites with mild dysplasia may be at increased risk of progression compared to other mild dysplasia sites with fewer optical and genetic alterations. These findings suggest that optical markers may be a non-invasive alternative to gene expression analysis for clinical risk assessment.

Future research could also build upon this work. As all sites included in this study were from patients undergoing surgery for oral cancer, it could be informative to add sites with no dysplasia from subjects without oral cancer history to minimize the likelihood of field cancerization effects influencing optical and/or genetic properties identified from these samples. Only ventral tongue and lateral tongue sites were included in this study, and subsequent exploration, including buccal mucosa, gingiva, floor of mouth, and lip sites, could contribute to an understanding of alterations in optical properties and gene expression from a broader range of anatomic locations. Additionally, the collection of longitudinal data would facilitate a direct analysis of whether low- grade dysplasia sites with abnormal optical properties and modulated gene expression ultimately exhibited increased progression and malignant transformation rates.

Conclusions

In sum, this study suggests that high-resolution imaging can identify oral lesions with mild dysplasia that are undergoing the genetic changes that drive oral carcinogenesis. Integration of these optical imaging diagnostic adjuncts into the clinical workflow could provide clinicians with additional information to assist with the identification, evaluation, and management of potentially premalignant oral sites.

Citation diversity

Recent work in several fields of science has identified a bias in citation practices such that papers from women and other minority scholars are undercited relative to the number of papers in the field [26–29]. We recognize this bias and have worked diligently to ensure that we are referencing appropriate papers with fair gender and racial author inclusion.

Supplementary Material

Refer to Web version on PubMed Central for supplementary material.

Acknowledgments

Timothy Quang, Katelin D. Cherry, Eric C. Yang, Imran S. Vohra, Hawraa Badaoui, and Alex Kortum conducted the imaging for patients in this study.

Funding

Research reported in this publication was supported by the National Institutes of Health under award number R01DE029590 (to RR Richards-Kortum). Slide preparation was performed by the MD Anderson Research Histology Core Laboratory supported by the National Cancer Institute of the National Institutes of Health under award number P30CA016672. Research supported by the National Cancer Institute under the immunotherapy “moonshot” award number 1U01DE028233-01 (to Andrew Sikora).

References

[1]. Bray F, Ferlay J, Soerjomataram I, Siegel RL, Torre LA, Jemal A. Global cancer statistics 2018: GLOBOCAN estimates of incidence and mortality worldwide for 36 cancers in 185 countries. CA Cancer J Clin 2018;68(6):394–424. [PubMed: 30207593]

[2]. National Cancer Institute. Bethesda M. SEER Cancer Stat Facts: Oral Cavity and Pharynx Cancer [Internet]. Available from: https://seer.cancer.gov/statfacts/html/oralcav.html.

[3]. Warnakulasuriya S, Kovacevic T, Madden P, Coupland VH, Sperandio M, Odell E, et al. Factors predicting malignant transformation in oral potentially malignant disorders among patients accrued over a 10-year period in South East England.J Oral Pathol Med 2011;40(9):677–83. [PubMed: 21762430]

[4]. Brennan M, Migliorati CA, Lockhart PB, Wray D, Al-Hashimi I, Axéll T, et al. Management of oral epithelial dysplasia: a review. Oral Surgery, Oral Med Oral Pathol Oral Radiol Endodontology 2007;103:S19–21.

[5]. Dionne KR, Warnakulasuriya S, Binti Zain R, Cheong SC. Potentially malignant disorders of the oral cavity: Current practice and future directions in the clinic and laboratory. Int J Cancer 2015;136(3):503–15. [PubMed: 24482244]

[6]. Lingen MW, Abt E, Agrawal N, Chaturvedi AK, Cohen E, D’Souza G, et al. Evidence- based clinical practice guideline for the evaluation of potentially malignant disorders in the oral cavity: a report of the American Dental Association. J Am Dent Assoc 2017;148(10):712–27. [PubMed: 28958308]

[7]. Wu C, Gleysteen J, Teraphongphom NT, Li Y, Rosenthal E. In-vivo optical imaging in head and neck oncology: basic principles, clinical applications and future directions. Int J Oral Sci 2018;10(2):1–13. [PubMed: 29343681]

[8]. Pierce MC, Schwarz RA, Bhattar VS, Mondrik S, Williams MD, Lee JJ, et al. Accuracy of In Vivo Multimodal Optical Imaging for Detection of Oral Neoplasia. Cancer Prev Res 2012 Jun;5(6):801–9.

[9]. Quang T, Tran EQ, Schwarz RA, Williams MD, Vigneswaran N, Gillenwater AM, et al. Prospective Evaluation of Multimodal Optical Imaging with Automated Image Analysis to Detect Oral Neoplasia In Vivo. Cancer Prev Res 2017 Oct;10(10): 563–70.

[10]. Yang EC, Vohra IS, Badaoui H, Schwarz RA, Cherry KD, Jacob J, et al. Prospective evaluation of oral premalignant lesions using a multimodal imaging system: a pilot study. Head Neck 2020;42(2):171–9. [PubMed: 31621979]

[11]. Romano A, Di Stasio D, Petruzzi M, Fiori F, Lajolo C, Santarelli A, et al. Noninvasive imaging methods to improve the diagnosis of oral carcinoma and its precursors: State of the art and proposal of a three-step diagnostic process. Cancers (Basel) 2021;13(12):2864. [PubMed: 34201237]

[12]. Poh CF, Zhang L, Anderson DW, Durham JS, Williams PM, Priddy RW, et al. Fluorescence visualization detection of field alterations in tumor margins of oral cancer patients. Clin Cancer Res 2006;12(22):6716–22. [PubMed: 17121891]

[13]. Bugter O, Spaander MCW, Bruno MJ, de Jong RJB, Amelink A, Robinson DJ. Optical detection of field cancerization in the buccal mucosa of patients with esophageal cancer. Clin Transl Gastroenterol 2018;9(4).

[14]. Hanahan D, Weinberg RA. Hallmarks of cancer: the next generation. Cell 2011;144 (5):646–74. [PubMed: 21376230]

[15]. Geiss GK, Bumgarner RE, Birditt B, Dahl T, Dowidar N, Dunaway DL, et al. Direct multiplexed measurement of gene expression with color-coded probe pairs. Nat Biotechnol 2008;26(3):317–25. [PubMed: 18278033]

[16]. Ran D, Moharil J, Lu J, Gustafson H, Culm-Merdek K, Strand-Tibbitts K, et al. Platform comparison of HTG EdgeSeq and RNA-Seq for gene expression profiling of tumor tissue specimens. American Society of Clinical Oncology; 2020.

[17]. Qi Z, Wang L, Desai K, Cogswell J, Stern M, Lawson B, et al. Reliable gene expression profiling from small and hematoxylin and eosin–stained clinical formalin-fixed, paraffin-embedded specimens using the HTG EdgeSeq Platform. Mol Diagnostics 2019;21(5):796–807.

[18]. Muldoon TJ, Pierce MC, Nida DL, Williams MD, Gillenwater A, Richards-Kortum R. Subcellular-resolution molecular imaging within living tissue by fiber microendoscopy. Opt Express 2007;15(25):16413–23. [PubMed: 19550931]

[19]. Yang EC, Vohra IS, Badaoui H, Schwarz RA, Cherry KD, Quang T, et al. Development of an integrated multimodal optical imaging system with real-time image analysis for the evaluation of oral premalignant lesions. J Biomed Opt 2019 Feb;24(2):1–10.

[20]. Barnes L, Eveson J, Reichart P, Sidransky D, others. World Health Organization classification of tumours: pathology and genetics of head and neck tumours; 2005.

[21]. Quang T, Schwarz RA, Dawsey SM, Tan MC, Patel K, Yu X, et al. A tablet-interfaced high-resolution microendoscope with automated image interpretation for real-time evaluation of esophageal squamous cell neoplasia. Gastrointest Endosc 2016;84(5): 834–41. [PubMed: 27036635]

[22]. McCarthy DJ, Chen Y, Smyth GK. Differential expression analysis of multifactor RNA-Seq experiments with respect to biological variation. Nucleic Acids Res 2012; 40(10):4288–97. [PubMed: 22287627]

[23]. Benjamini Y, Hochberg Y. Controlling the false discovery rate: a practical and powerful approach to multiple testing. J R Stat Soc Ser B 1995;57(1):289–300.

[24]. Zhou Y, Zhou B, Pache L, Chang M, Khodabakhshi AH, Tanaseichuk O, et al. Metascape provides a biologist-oriented resource for the analysis of systems-level datasets. Nat Commun 2019;10(1):1–10. [PubMed: 30602773]

[25]. Odell E, Kujan O, Warnakulasuriya S, Sloan P. Oral epithelial dysplasia: Recognition, grading and clinical significance. Oral Dis 2021.

[26]. Caplar N, Tacchella S, Birrer S. Quantitative evaluation of gender bias in astronomical publications from citation counts. Nat Astron 2017;1(6):141.

[27]. Dworkin JD, Linn KA, Teich EG, Zurn P, Shinohara RT, Bassett DS. The extent and drivers of gender imbalance in neuroscience reference lists. bioRxiv [Internet]. 2020; Available from: https://www.biorxiv.org/content/early/2020/01/11/2020.01.03.894378.

[28]. Maliniak D, Powers R, Walter BF. The gender citation gap in international relations. Int Organ 2013;67(4):889–922.

[29]. Dion ML, Sumner JL, Mitchell SM. Gendered citation patterns across political science and social science methodology fields. Polit Anal 2018;26(3):312–27.

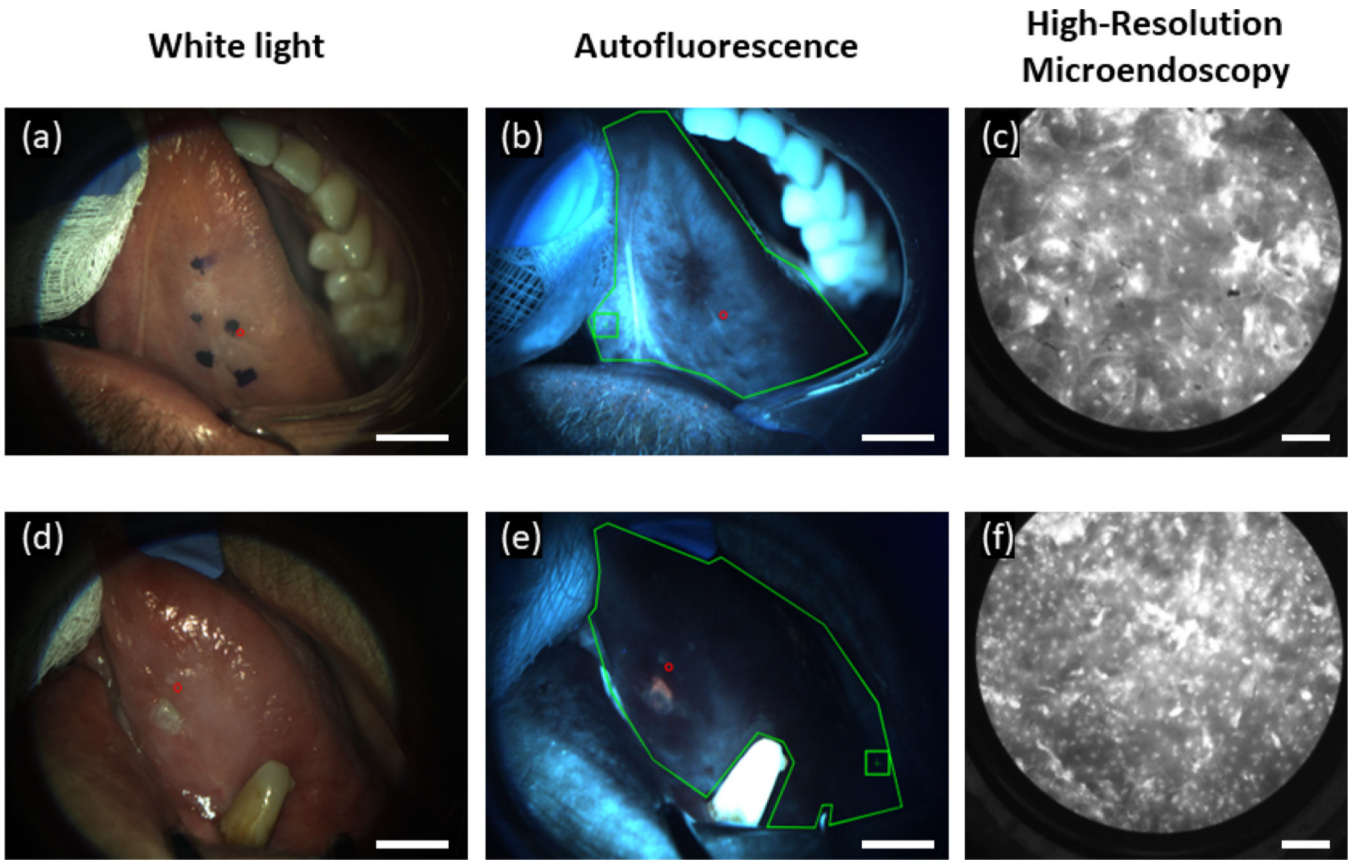

Fig. 1.

Multimodal optical images from the oral cavity of two patients with clinically 'abnormal not suspicious' sites that contained histologically confirmed mild dysplasia. (a-c) Images of the ventral tongue of Patient 1. (a) Widefield, white light image and (b) corresponding widefield autofluorescence image with site of interest indicated by a red circle. The normalized red-to-green autofluorescence ratio at the site was 1.15. (c) Corresponding high-resolution microendoscopy image of Patient 1 with 153.1 abnormal nuclei/mm^2. (d-f) Images of the ventral tongue of Patient 2. (d) Widefield, white light image and (e) corresponding widefield autofluorescence image with site of interest indicated by a red circle. The red-to-green autofluorescence ratio at the site was 1.81. (f) Corresponding high-resolution microendoscopy image of Patient 2 with 226.8 abnormal nuclei/mm^2. In the autofluorescence images the green outline denotes the oral mucosa while the green square encompasses the area used for normalizing the red-to-green ratio. Scale bar in high-resolution microendoscopy images represents 100 μm. Scale bar in the widefield images represents 1 cm. (For interpretation of the references to color in this figure legend, the reader is referred to the web version of this article.)

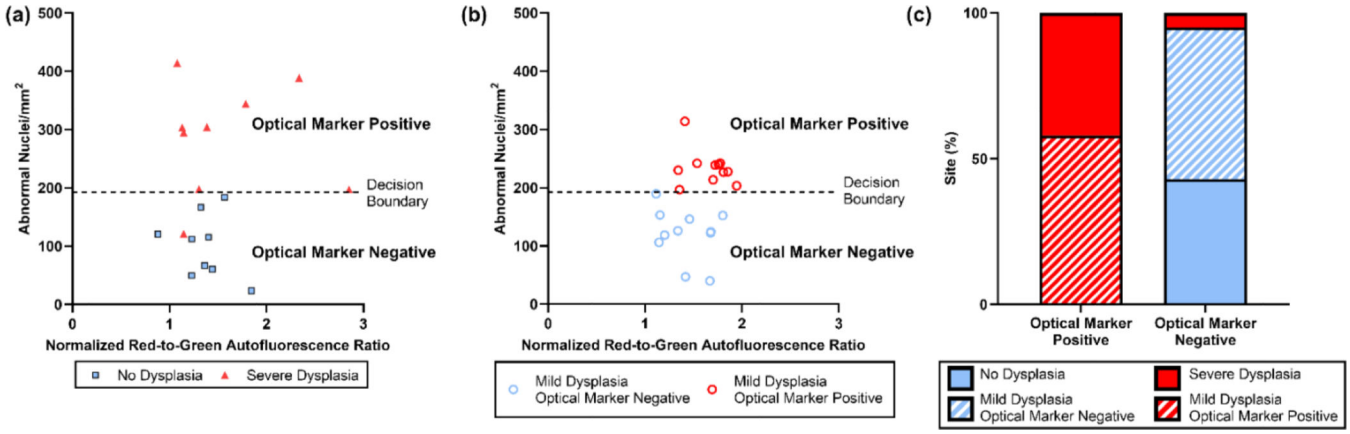

Fig. 2.

Characterization of sites based on optical markers. (a) Sites with no dysplasia had lower values of optical markers, while sites with severe dysplasia had higher values of optical markers. Nearest centroid classification was used to define a decision boundary between sites with no dysplasia and sites with severe dysplasia. (b) Sites with mild dysplasia were divided into two categories based on the decision boundary: optical marker negative or optical marker positive. (c) Sites that were optical marker negative included all sites with no dysplasia and only one site with severe dysplasia; sites that were optical marker positive included all but one site with severe dysplasia. Sites with mild dysplasia were roughly evenly distributed in the two groups.

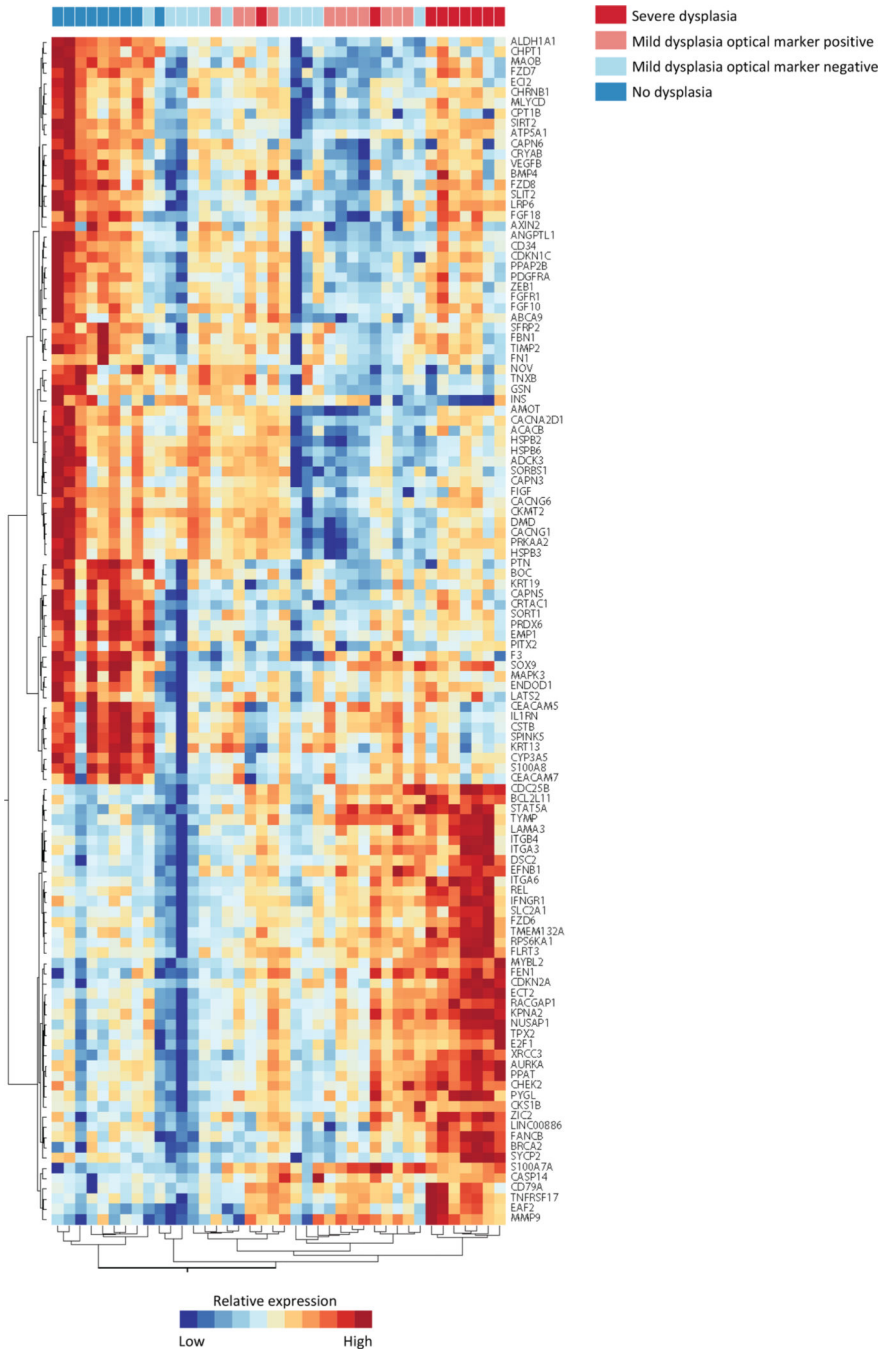

Fig. 3.

Clustering analysis of differential gene expression. Expression of genes differentially expressed between groups with no dysplasia and severe dysplasia (adjusted p-value < 0.01) examined across all samples. Hierarchical clustering analysis was performed on genes and samples. Heatmap scale for relative expression range corresponds to range within each individual gene.

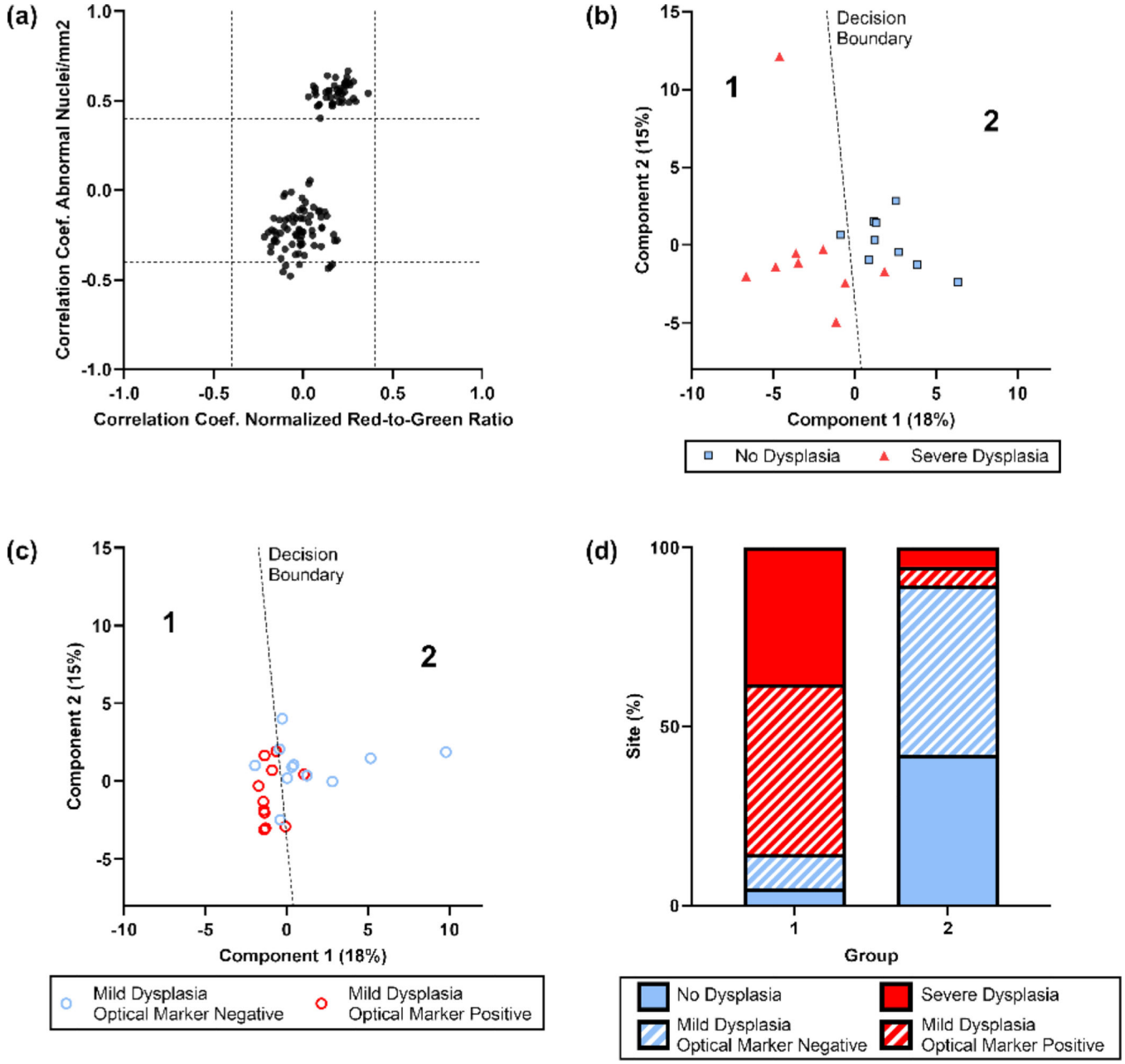

Fig. 4.

Identification and characterization of differentially expressed genes strongly correlated to optical marker values. (a) Pearson coefficients for correlation of optical markers (abnormal nuclei/mm2 and normalized red-to-green ratio) to the expression of the 116 differentially expressed genes between groups with no dysplasia and severe dysplasia. Fifty genes were strongly correlated to the value of abnormal nuclei/mm2 (Pearson coefficient ≤ −0.4 or ≥ 0.4). (b) Nearest centroid classification applied to the principal component analysis of the expression of 50 strongly correlated genes separated sites with no dysplasia and sites with severe dysplasia. (c) Principal component analysis of the expression of 50 strongly correlated genes sites with mild dysplasia. The decision boundary separated sites with mild

dysplasia into two groups: 1) a group with gene expression similar to sites with severe dysplasia, and 2) a group with gene expression similar to sites with no dysplasia. (d) Distribution of histologic diagnoses for sites based on decision boundary shown in Fig. 4b. Most sites with mild dysplasia and positive optical markers grouped with the majority of severe dysplasia sites. Most sites with mild dysplasia and negative optical markers grouped with the majority of sites with no dysplasia. (For interpretation of the references to color in this figure legend, the reader is referred to the web version of this article.)

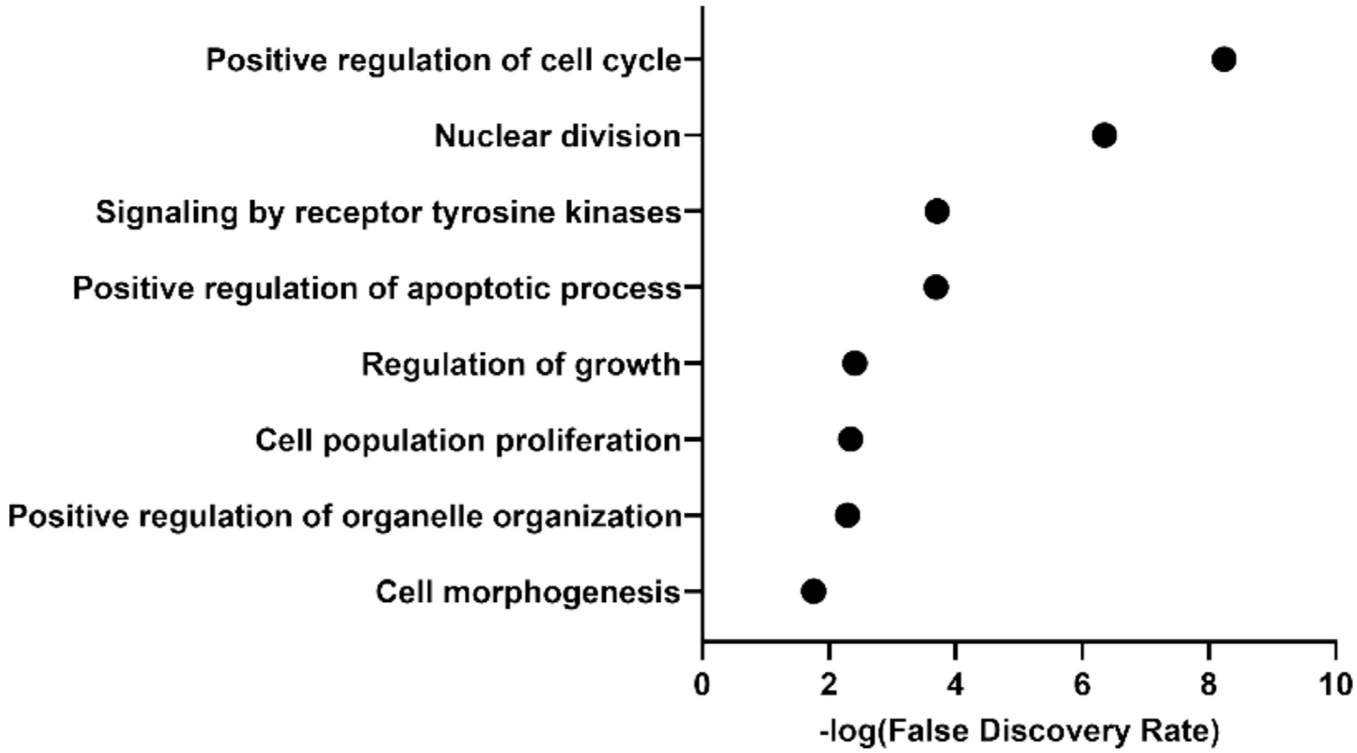

Fig. 5.

Top parent terms associated with the 50 genes strongly correlated to the abnormal nuclei/mm2 optical marker.

Table 1

Pathology diagnosis and clinical impression of 40 sites selected for optical marker and gene expression analysis.

Pathology	Clinical Impression	No. of Sites
No dysplasia		*9*
	Normal	4
	Abnormal not suspicious	5
Mild dysplasia		22
	Normal	5
	Abnormal not suspicious	6
	Abnormal suspicious	9
	Cancer	2
Severe dysplasia		9
	Normal	1
	Abnormal suspicious	8